Synthesis of Polymer-coated Magnetic Nanoparticles

Tania Dey* and Charles J. O'Connor

Advanced Materials Research Institute, 2000 Lakeshore Drive, University of New Orleans, New Orleans, Louisiana 70148

* Corresponding Author. E-mail: taniadey@hotmail.com

ABSTRACT

ATRP (atom transfer radical polymerization) approach was employed to synthesis polymer-coated magnetite nanoparticles with an average diameter of 7.1 nm and of narrow size distribution, followed by various characterization techniques like Transmission Electron Microscopy (TEM), Ultraviolet-Visible spectroscopy (UV-vis), Fourier Transform Infrared spectroscopy (FTIR) and Atomic Force Microscopy (AFM). The challenge was to obtain a thin shell and particles in an unagglomerated state. Several factors like presence/choice of solvent, monomer-to-initiator concentration and structure of initiator were found to play a key role in this study. Attempts have been made to tailor the polymer shells by end-functionalization. This work has an enormous biomedical application potential.

Keywords: magnetite nanoparticles, polystyrene, atom transfer radical polymerization, capping ligand

1 INTRODUCTION

The formation of polymeric shell is essential for biomedical application of magnetic nanoparticles such as targeted drug delivery, magnetic resonance imaging (MRI) contrast enhancement, biosensors, protein and DNA purification, cell separation and so on. In these applications, good control over particle size, size distribution and surface properties are important. Atom transfer radical polymerization (ATRP) is a versatile method which offers several advantages over other polymerization techniques including good control over molecular weight and polydispersity. Lot of work has been done in the area of in-situ preparation of nanoparticle-polymer hybrids using polymer as a matrix to obtain an array of embedded nanoparticles, but to obtain discrete polymer-coated nanoparticle still remains as a challenge. Some ATRP approaches were reported to make core-shell systems including various inorganic cores like SiO_2, Au, $MnFe_2O_4$, $Au@SiO_2$ and Fe_2O_3 [1-8], but no attempt has been made so far that involves magnetite nanoparticles, which shows strong ferrimagnetic behavior and is less susceptible towards oxidation in comparison to other magnetic transition metals.

We have synthesized spherical magnetite (Fe_3O_4) nanoparticles with an average diameter of 5.6 nm and a narrow size distribution, by co-precipitating iron (II) and iron (III) chloride salts in presence of sodium hydroxide at elevated temperature. Long chain carboxylic acid were found to stabilize these nanoparticles and act as a capping ligand [9]. We have obtained polystyrene coated magnetite nanoparticles of average diameter < 10 nm by a two-step process: firstly modifying the surface of nanoparticles with initiator and then using these initiator-exchanged nanoparticles as a macroinitiator for copper-mediated ATRP reaction. Systems were characterized by TEM, UV-vis, FTIR, AFM and GPC. Choice of initiator, solvent and monomer-to-initiator concentration ratio were found to play a key role in our study. Recent efforts have been made to impart dispersity and stability to magnetite nanoparticles by polymer-coating [10,11]; but polymerization may not be considered as a method of preventing agglomeration only. The potential lies in the tailorability of these polymer shells as it maybe end-functionalized or block-copolymerized.

2 EXPERIMENTAL SECTION

2.1 Instrumentation

Transmission Electron Microscope. The TEM images were recorded on a JEOL Model 2010 at an accelerating voltage of 200 kV. The TEM specimens were made by placing a drop of toluene suspension of nanoparticles on formvar/carbon 200 mesh, copper grid (tedpella.com).
Atomic Force Microscope. AFM images were obtained from a Multimode Scanning Probe Microscope, Digital Instruments (Veeco metrology group).
UV-vis spectrometer. VARIAN Carey 500 scan UV-vis-NIR spectrophotometer was used to measure the absorption of nanoparticle solution taken in a quartz cell.
FT-IR spectrometer. The FT-IR spectra were collected on a Thermo-Nicolet NEXUS 670 FT-IR spectrometer using KBr pellets.

2.2 Synthesis

Synthesis of Magnetite Nanoparticle. 2 mmol of $FeCl_2.4H_2O$ and 4 mmol of $FeCl_3.6H_2O$ were dissolved in 40 g of diethylene glycol (DEG, Alfa Aesar, 99%) in a schlenk flask under protection with argon. Separately, 16 mmol of NaOH (EMD chemicals, GR) was dissolved in 40 g DEG. The solution of NaOH was added to the solution of metal chlorides while stirring at room temperature causing an immediate color change. The temperature of the resulting solution was raised during 1-1.5 h to 210-220 ^oC and then kept constant for 0.5-1 h. As the solution turned turbid, the reaction was terminated by adding 2.6 mmol of oleic acid (Aldrich, 90%) dissolved in 20 g of DEG. This addition caused immediate precipitation of solid particles. The mixture was cooled at room temperature and then centrifuged. The precipitate was washed with molecularly sieved methanol for several times. The yield of black powder was 0.65 g.

Synthesis of Polystyrene coating. The prepared Fe_3O_4 nanoparticles were dispersed in 1.0 M hexane solution of the initiator, 2-bromo-2-methyl propionic acid (Br-MPA) (Aldrich 98%) and stirred for 72 h at room temperature under protection of argon. The resulting powder was separated using a centrifuge, washed with hexane to remove the excess initiator and was dried under vacuum. The initiator-exchanged nanoparticles (0.055g) were added into 2mL of argon-purged styrene solution (Aldrich, 99+%). CuBr (0.3 mmol, Aldrich, 98%) and 4,4'-dinonyl-2,2'-dipyridyl (1.1 mmol, Aldrich, 97%) were dissolved in 4 mL of xylene (Aldrich, AR) and then the solution was added to the styrene/nanoparticle mixture. The final solution was stirred and kept at 100 ^oC for 20 h. On completion of reaction, the mixture was 10 times diluted with tetrahydrofuran (THF, Aldrich 99%), centrifuged and washed with methanol.

3 RESULTS AND DISCUSSION

One of the fundamental characterization tools used in this work was TEM. Figure 1 shows the TEM images of oleic acid stabilized well dispersed Fe_3O_4 nanoparticles, as well as the initiator-exchanged and polystyrene-coated Fe_3O_4 nanoparticles. A change in morphology from spherical to faceted ones was observed due to initiator-exchange. A dark center surrounded by a light shell was visible under the microscope upon polymerization. Particle sizes and shell thickness were determined by manually counting over 100 particles. The core/shell nanoparticles showed an average diameter of 7.1 nm, whereas the nanoparticles itself had an average diameter of 5.6 nm, both having a narrow size distribution (as shown in Figure 2).

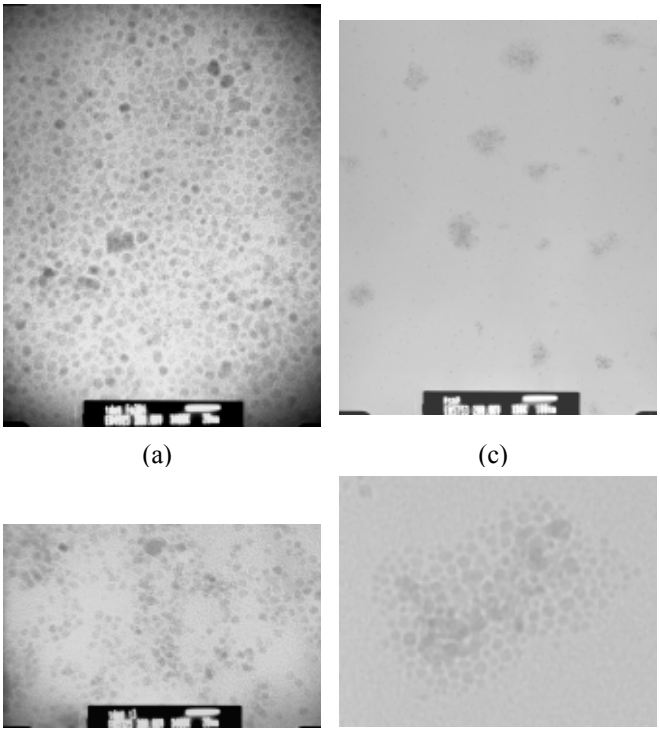

(a) (c)

(b) (d)

Figure 1: TEM images **(a)** Fe_3O_4 nanoparticles **(b)** initiator-exchanged nanoparticles **(c)** poly styrene-coated nanoparticles **(d)** one portion of (c) is enlarged

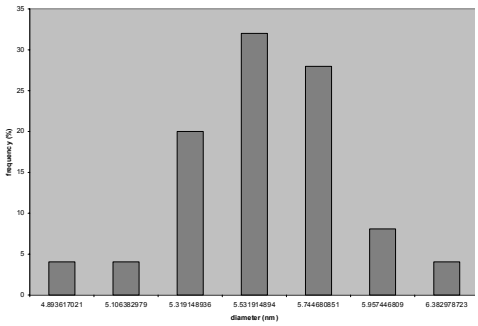

(a)

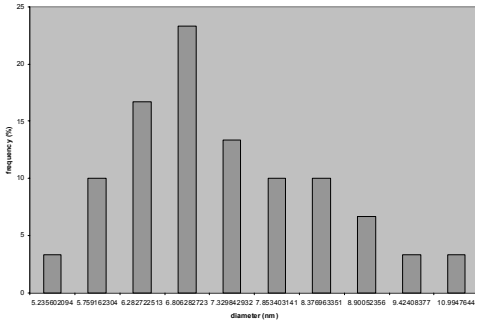

(b)

Figure 2: Size distribution of **(a)** Fe_3O_4 nanoparticles **(b)** polystyrene-coated nanoparticles

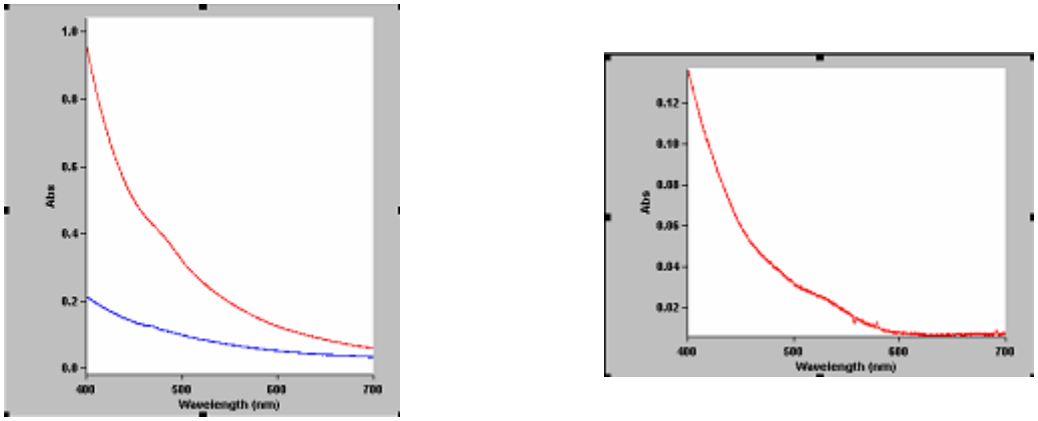

(a) (b)

Figure 3: (a) UV-vis spectra of Fe_3O_4 nanoparticle before and after initiator exchange **(b)** UV-vis spectrum of Fe_3O_4-polystyrene nanoparticle

The clear yellow ethanolic suspension of initiator-exchanged nanoparticle displayed a broad plasmon absorption band at 475 nm indicative of iron oxide, just like the nanoparticles before capping ligand exchange (Figure 3a). A red-shift was observed upon polymerization which may be attributed due to decrease in inter-particle distance caused by increased size, although no precipitation/ aggregation was observed (Figure 3b).

The alkyl C-H vibration bands in the IR spectra (Figure 4a) suggested that there was an equilibrium in the ligand-exchange process. However the occurance of the relatively stronger peaks of CH_3 groups after initiator-exchange was consistent with the fact that CH_3 was the major alkyl group in Br-MPA, while oleic acid predominantly had CH_2 groups. The existence of macroinitiator was also supported by the IR band at 1010 cm^{-1} belonging to Br-MPA. Characteristic peaks of polystyrene at 2700-3500, 1000-1400 and 700 cm^{-1} (Figure 4b) were observed in the core-shell samples indicating polymerization.

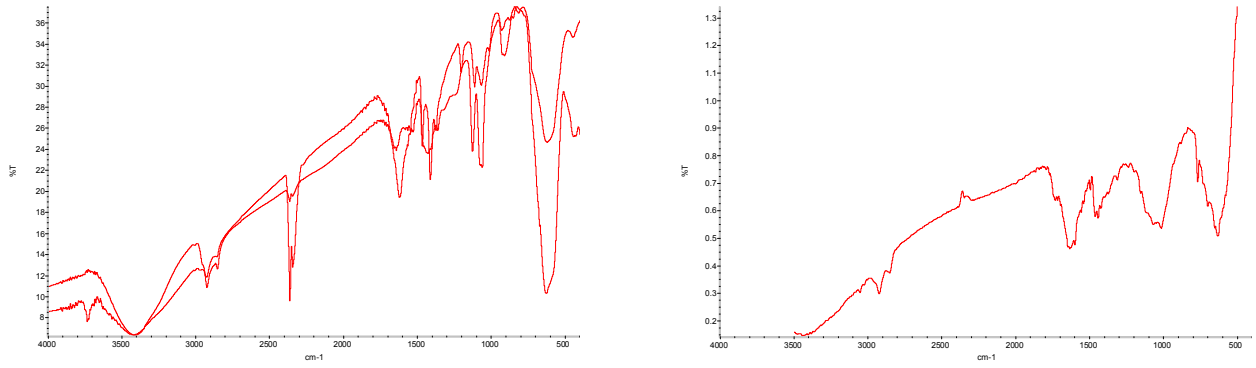

(a) (b)

Figure 4: (a) FTIR spectra of Fe_3O_4 exchange **(b)** FTIR spectrum of polystyrene nanoparticle before and after initiator -coated nanoparticle

The tapping mode AFM measurements (Figure 5) verified the successful grafting of polymer on nanoparticles and was in good agreement with the particle size obtained from TEM. The morphology and volume of hybrid nanoparticles can also be determined by this method, complementing the TEM studies.

Ongoing studies include GPC measurements to obtain molecular weight and polydispersity of the polymeric shells, and the SQUID measurements to determine magnetic surface anisotropy and coercivity.

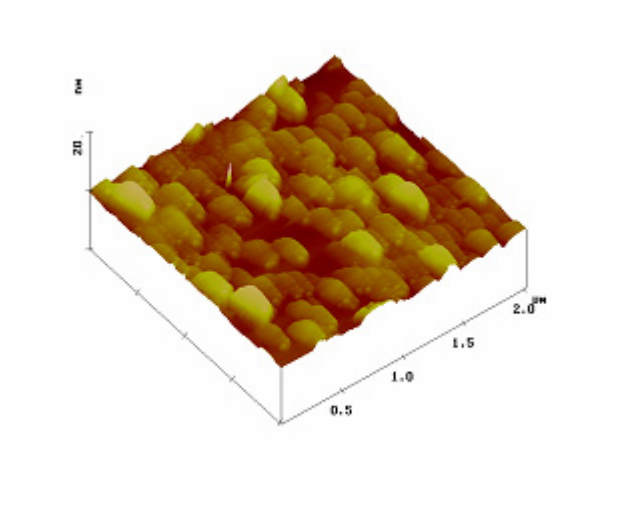

Figure 5: AFM image of polymer -coated nanoparticles

Presence of a solvent was found to be essential during polymerization to impart good dispersity, unlike the solvent-free approach where the initiator-exchanged as well as the polymer-coated nanoparticles were found to be kind of aggregated. Xylene proved to be the best candidate in this respect. Significant amount of work has been accomplished in varying the initiator structure by incorporating some hydrophobic moiety for better dispersity and choosing appropriate monomer to introduce end-functionalization for better anchoring of biomolecules (to be published elsewhere).

4 CONCLUSION

ATRP approach works very well to produce thin polystyrene shell (~1.5 nm) on magnetic Fe_3O_4 nanoparticles, which makes the system biologically interesting. The core-shell structures can be obtained in a fairly unaggregated state by controlling the presence/choice of solvent, monomer-to-initiator ratio and initiator structure. Polymer shells can be tuned to impart biocompatibility as well as biospecificity.

Acknowledgment. This work was supported by DARPA (Grant No. MDA972-02-1-0001).

REFERENCES

[1] J. Pyun and K. Matyjaszewski, Chem. Mater. *13,* 3436-3448, **2001.**
[2] T. von Werne and T. E. Patten, J. Am. Chem. Soc. *123,* 7497-7505, **2001.**
[3] K. Kamata, Y. Lu and Y. N. Xia, J. Am. Chem. Soc. *125,* 2384-2385, **2003.**
[4] C. R. Vestal and Z. J. Zhang, J. Am. Chem. Soc. *124,* 14312-14313, **2002.**
[5] K. Ohno, K. Koh, Y. Tsujii and T. Fukuda, Macromolecules *35,* 8989-8993, **2002.**
[6] T. K. Mandal, M. S. Fleming and D. R. Walt, Nano Lett. *2*, 3-7, **2002.**
[7] D. A. Savin, J. Pyun, G. D. Patterson, T. Kowalewski and K. Matyjaszewski, J. Polym. Sci. Part B: Polym. Phys. *40,* 2667-2676, **2002.**
[8] Y. Wang, X. Teng, J-S. Wang and H. Yang, Nano Lett. *3*, 789-793, **2003.**
[9] D. Caruntu, Y. Remond, N. H. Chou, M-J. Jun, G. Caruntu, J. He, G. Goloverda, C. O'Connor and V. Kolesnichenko, Inorg. Chem. *41*, 6137-6146, **2002.**
[10] R. Matsuno, K. Yamamoto, H. Otsuka and A. Takahara, Macrocolecules *37*, 2203-2209, **2004.**
[11] R. Matsuno, K. Yamamoto, H. Otsuka and A. Takahara, Chem. Mater. *15*, 3-5, **2003.**